



DFT study of the cohesive and structural properties of YNi_5H_x compounds



G.I. Miletić*, A. Drašner

Laboratory for Solid State and Complex Compounds Chemistry, Division of Materials Chemistry, Institute Rudjer Bošković, P.O. Box 180, 10002 Zagreb, Croatia

ARTICLE INFO

Article history:

Received 7 February 2014
Received in revised form 10 October 2014
Accepted 22 October 2014
Available online 29 October 2014

Keywords:

Intermetallics
Metal hydrides
Electronic band structure
Enthalpy
DFT calculations

ABSTRACT

YNi_5H_x compounds with $x = 0.0, 0.25, 0.5, 1.0, 3.0, 3.5, 4.0$ were investigated using density functional theory with ultrasoft pseudopotentials and a plane wave basis set. The formation energetics of the considered compounds was investigated, and the preference of H atoms for particular interstitial sites was explored. The enthalpy of formation of the β phase, through the reaction $\alpha \rightarrow \beta$, was calculated and a reasonable correspondence was found between theoretical values and a value that was previously obtained from experiment.

© 2014 Elsevier B.V. All rights reserved.

1. Introduction

Among the plethora of structures assumed by the intermetallic compounds, the so-called hexagonal Haucke phases (CaCu_5 structure) have attracted attention due to both their magnetic properties and for the purposes of hydrogen storage and its related applications [1,2]. Notable members of the group of hexagonal Haucke intermetallic compounds that exhibit the desirable hydrogen absorption properties are LaNi_5 and some LaNi_5 -based intermetallics [2,3].

The binary intermetallic compound YNi_5 has also attracted attention from the point of view of hydrogen absorption properties [4–10]. Investigations of the $\text{YNi}_5\text{-H}_2$ system [4–10] indicate that the stability of hydrides in the $\text{YNi}_5\text{-H}_2$ system is considerably lower than the stability of hydrides in the $\text{LaNi}_5\text{-H}_2$ system.

In order to investigate the stability of different atomic arrangements that could be realised when H atoms enter the YNi_5 crystal structure, density functional theory (DFT) calculations were performed for various model structures of YNi_5H_x ($x = 0.0, 0.25, 0.5, 1.0, 3.0, 3.5, 4.0$) compounds. More specifically, the investigations of the stability of the considered compounds included an investigation of the site preference of H atoms, the energetics of α solid solution formation and the energetics of the $\alpha \rightarrow \beta$ reaction.

2. Computational details

The DFT calculations were performed using plane waves (PW) as a basis set and ultrasoft (US) pseudopotentials (PP) [11,12] to describe the ion cores, as implemented in the QUANTUM ESPRESSO package [13].

Unless otherwise stated, the calculations included optimizations of crystal (and molecular for H_2) geometries and the presented results correspond to these relaxed structures.

All investigated YNi_5H_x compounds were treated with non-spin-polarized (NSP) calculations, unless stated otherwise. Y-hcp, Ni-fcc and the H_2 molecule were treated within spin-polarized (SP) calculations and, as expected, only Ni-fcc was found to be magnetic.

For the wavefunctions the plane wave cut-off was 35.0 Ry, while for the charge density and potential it was set to 350.0 Ry. Generalized gradient approximation (GGA) in the Perdew, Burke and Ernzerhof (PBE) form [14,15] was used for the calculation of the exchange–correlation energy.

For the modelling of hydrides YNi_5H_x with lower hydrogen contents ($x = 0.25, 0.5, 1.0$), neutron diffraction data obtained in [16] and given in Table S1 in the Supplementary data were used. The CaCu_5 structure with the five interstitial positions that were used to model hydrides with lower hydrogen contents in this work are shown in Fig. 1. Compositions $x = 1.0, 0.5$ and 0.25 were modelled using single ($1 \times 1 \times 1$), double ($1 \times 1 \times 2$) and quadruple ($2 \times 2 \times 1$) CaCu_5 -type unit cells with one H atom, respectively. Although the symmetry will be, in general, lowered after the insertion of a

* Corresponding author. Tel.: +385 1 4561 111; fax: +385 1 468 0084.

E-mail address: gmiletic@irb.hr (G.I. Miletić).

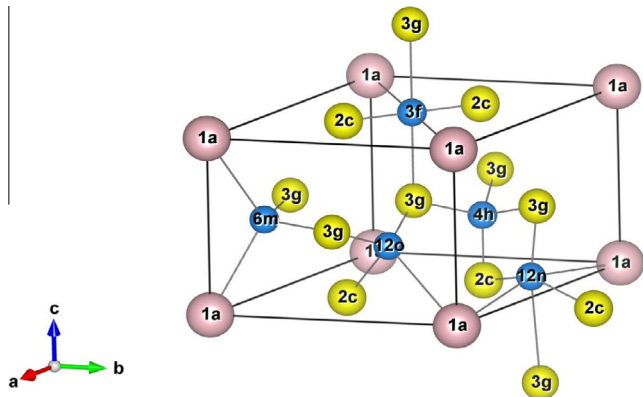


Fig. 1. CaCu_5 structure with five interstitial positions [16]. Rose, yellow and blue spheres correspond to the Ca-like atoms, Cu-like atoms and interstitial positions (or H atoms), respectively. The figure was produced with the VESTA programme [72]. (For interpretation of the references to colour in this figure legend, the reader is referred to the web version of this article.)

H atom into the YNi_5 structure, the interstitial positions will be labelled as if the original space group of the intermetallic compound YNi_5 ($P6/mmm$) is conserved.

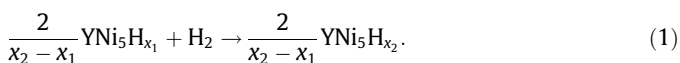
We also note that in this work we use the two formulae $\text{R}_n\text{Ni}_{5n}\text{H}_x$ and RNi_5H_x interchangeably.

Hydrides with higher hydrogen contents ($x \geq 3.0$) were modelled using crystal structure parameters obtained from neutron diffraction experiments for $\beta^I\text{-LaCo}_5\text{D}_{3.35}$ (see Table S2) and $\beta^{III}\text{-CeCo}_5\text{D}_{2.55}$ phase (see Table S3) [17]. Unit cells of the $\beta^I\text{-LaCo}_5\text{D}_{3.35}$ and $\beta^{III}\text{-CeCo}_5\text{D}_{2.55}$ phases are given in Figs. 2 and 3, respectively. Unless stated otherwise, the results reported for compounds with $x \geq 3.0$ are those corresponding to the crystal structures derived on the basis of the $\beta^I\text{-LaCo}_5\text{D}_{3.35}$ phase [17].

Brillouin zone (BZ) integrations were performed using Monkhorst–Pack [18] \mathbf{k} -point meshes along with the Marzari–Vanderbilt (MV) cold-smearing (CS) method [19] with a broadening of 0.01 Ry.

For BZ integrations, $12 \times 12 \times 12$ \mathbf{k} -meshes, or appropriately reduced \mathbf{k} -meshes, were used for single or multiple CaCu_5 -like unit cells, respectively. For hydrides that were modelled using crystal structure data determined for the $\beta^I\text{-LaCo}_5\text{D}_{3.35}$ phase [17], $13 \times 12 \times 12$ (see footnote¹) and $6 \times 10 \times 14$ \mathbf{k} -meshes were used for the primitive (one YNi_5 f.u./unit cell) and conventional (two YNi_5 f.u./unit cell) unit cells, respectively. In the case of the YNi_5H_3 composition that was modelled with the structure isostructural to the $\beta^{III}\text{-CeCo}_5\text{D}_{2.55}$ phase [17], a $12 \times 12 \times 6$ \mathbf{k} -mesh was used for primitive unit cell (two YNi_5 f.u./unit cell). The Y-hcp and Ni-fcc \mathbf{k} -meshes employed in the calculations were $20 \times 20 \times 10$ and $20 \times 20 \times 20$, respectively. For calculation on the H_2 molecule a cubic box with sides 20.0 a.u. \times 20.0 a.u. \times 20.0 a.u. was used, and the calculation was performed solely for the Γ point of the BZ.

Depending on the context, different notations for the enthalpy of formation were used in this work. The enthalpy of formation of chemical species C , $\Delta H(C)$, through reaction $A + B \rightarrow C$ is calculated as $\Delta H(C) = E(C) - (E(A) + E(B))$, where $E(X)$ is the total energy of chemical species X . On the other hand, the enthalpy of formation denoted as $\Delta H_{x_1 \rightarrow x_2}$ applies to the following reaction [20],



¹ $13 \times 12 \times 12$ \mathbf{k} -mesh corresponds to the reciprocal lattice that is constructed from the direct primitive lattice parameters given in the following order: c , a and $b = a$ i.e. lattice parameters are exchanged relative to the usual convention. Results with these exchanged lattice parameters are given in Table S7 in the Supplementary data.

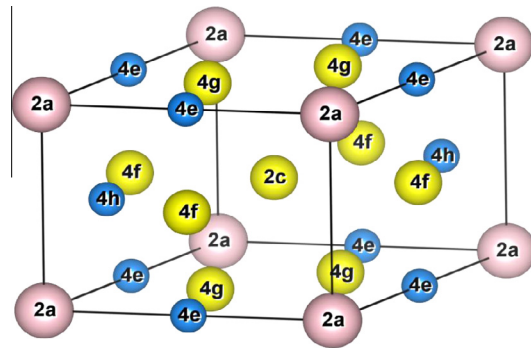


Fig. 2. $\beta^I\text{-LaCo}_5\text{H}_{3.35}$ structure [17]. Rose, yellow and blue spheres correspond to the La-like, Co-like and H atoms, respectively. The figure was produced with the VESTA programme [72]. (For interpretation of the references to colour in this figure legend, the reader is referred to the web version of this article.)

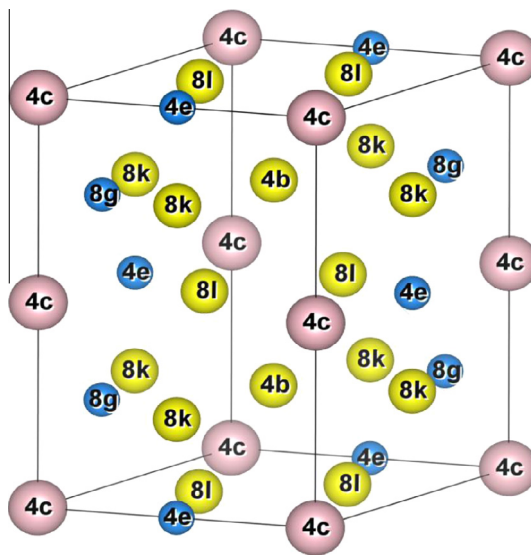


Fig. 3. $\beta^{III}\text{-CeCo}_5\text{H}_{2.55}$ structure [17]. Rose, yellow and blue spheres correspond to the Ce-like, Co-like and H atoms, respectively. The figure was produced with the VESTA programme [72]. (For interpretation of the references to colour in this figure legend, the reader is referred to the web version of this article.)

In the following, if the meaning is clear from the context the notation $\Delta H_{x_1 \rightarrow x_2}$ is abbreviated with ΔH or ΔE . Unless stated otherwise, contributions from zero-point energies (ZPE) are not included in the calculated enthalpies of formation.

3. Results and discussion

3.1. Intermetallic compound YNi_5

Results of the present US-PP-GGA calculations on YNi_5 are given in Table 1, along with previously obtained experimental and theoretical results.

The experimental and theoretical studies on YNi_5 are numerous and the set of references given in Table 1 is certainly not complete. Without aiming to give a complete set of references of the electronic structure calculations on YNi_5 and its related hydrides we note that, apart from the references given in Table 1, additional electronic structure calculations on YNi_5 and related hydrides include also [21–30]. Different computational approaches were used for the calculations, namely the full potential (FP) linear muffin-tin orbital (LMTO) method with the local density approximation (LDA) in [21,22], FP-LMTO-LDA and LMTO in the atomic sphere

Table 1

Results obtained from non-spin-polarized (NSP) and spin-polarized (SP) calculations for intermetallic compound YNi₅. Some previous experimental (exp.) and theoretical (theo.) results are also given. Enthalpy of formation, $\Delta H(\text{YNi}_5)$, applies to the reaction $\text{Y} + 5\text{Ni} \rightarrow \text{YNi}_5$. NSP and SP values of $\Delta H(\text{YNi}_5)$ were obtained from, NSP and SP values of the total energy of YNi₅, respectively, while for both (NSP and SP) cases the total energies of Y and Ni were obtained from SP calculations. Additional abbreviations: PM-paramagnetic.

YNi ₅	Present results		Previous results	
	NSP	SP	Exp.	Theo.
<i>a</i> (Å)	4.889	4.893	4.869 [10]	4.876 [31–34], 4.800 [35–37], 4.86310 [38]
<i>c</i> (Å)	3.956	3.964	3.972 [10]	3.950 [31–34], 4.094 [35–37], 3.94927 [38]
<i>M</i> _{spin} (μ _B /f.u.)	–	1.63	PM [39], PM [40], PM [41], PM [44]	1.5073 [31–34], 1.720 [35–37], 1.513 [38], 0 [42], 0 [43], 0 [45], 0.17 [46]
$\Delta H(\text{YNi}_5)$ (kJ/(mol YNi ₅))	–181.2	–185.9	–204.6 [47], –127.7 [48]	–186.5 [31–34], –201.3 [38], –211.2 [47], –156 [49]

approximation (ASA) with LDA in [23], pseudopotentials with GGA in [24], LMTO-ASA-LDA in [28] and the discrete variational (DV)-X α cluster method in [25–27,29,30].

From Table 1 it can be seen that there is good agreement between the lattice parameters of YNi₅ as previously obtained from experiment [10] with the data obtained from our calculations. Previous theoretical values [31–38] are mainly in good agreement with previous experimental [10] values and our theoretical values.

It may be noted that there is a significant difference between the two experimental values of the enthalpy of formation of YNi₅, $\Delta H(\text{YNi}_5)$, that were given in [47] and [48]. The value of $\Delta H(\text{YNi}_5) = -204.6$ kJ/(mol YNi₅) [47] seems to agree better than the value of -127.7 kJ/(mol YNi₅) [48] with the values obtained from our DFT calculations (-181.2 (-185.9) kJ/(mol YNi₅) for NSP (SP) calculations), and previous ones, with -186.5 kJ/(mol YNi₅) (projector augmented wave (PAW)-GGA method) [31–34] and -201.3 kJ/(mol YNi₅) (PAW-GGA) [38]. The semiempirical tight-binding (TB) Hartree-Fock (HF) approach was used in [47] and the calculated value was -211.2 kJ/(mol YNi₅), in a fair agreement with the values obtained from our and previous [31–34,38] DFT calculations, and an experimental value of -204.6 kJ/(mol YNi₅) [47]. Besides DFT and semiempirical TB-HF approaches, the Miedema model [50,51] was also employed for the calculation of the enthalpy of formation of YNi₅, and the obtained value was -156 kJ/(mol YNi₅) [49]. This is seemingly too high when compared with present and previous theoretical [31–34,38,47] results, as well as the previous experimental result [47]. On the other hand, the other experimental value [48] is somewhat higher than the value Niessen et al. [49] obtained using the Miedema model [50,51].

According to the experimental investigations of the magnetic properties of YNi₅, this compound is paramagnetic [39–41,44]. While in present calculations it was found that a magnetic state is more stable than a nonmagnetic state, with a spin magnetic moment of 1.63 μ_B/f.u., previous DFT calculations resulted in both nonmagnetic [42,43,45] and magnetic [31–38,46] states. More precisely, a solution with zero magnetic moment was obtained in the previous LMTO-ASA-LSDA (LSDA-local spin density approximation) [42], TB-LMTO-ASA-LSDA [43] and FP-LMTO-LSDA calculations [45], while a magnetic solution was obtained in the previous PAW-GGA [31–38] and KKR-ASA-LSDA (KKR-Korringa-Kohn-Rostoker) [46] calculations.

The spin magnetic moment of 1.63 μ_B/f.u. obtained in the present work agrees well with the former values of 1.5073 μ_B/f.u. [31–34], 1.720 μ_B/f.u. [35–37] and 1.513 μ_B/f.u. [38] while the former value of 0.17 μ_B/f.u. [46] seems to be somewhat too low when compared with the present value and other theoretical values given in [31–38].

3.2. YNi₅H_x (*x* = 0.25, 0.5, 1.0) compounds and the stability of the α -solid solution

In the CaCu₅ structure there are three different crystallographic positions which accommodate metal atoms, and it is generally accepted that there are five (3f, 4h, 12o, 12n and 6m) [16,52–54]

or six (3f, 4h, 12o, 12n, 6m and 6i) [55–57] interstitial crystallographic positions that should be considered as possible locations for hydrogen atoms. It should be noted that among the six positions, three of them (3f, 12n and 6i) are very close to one another in LaNi₅H_x compounds [55–57]. They are related as follows: 3f (1/2, 0, 0) → 6i (1/2, 0, z_{6i}) → 12n (x_{12n}, 0, z_{12n}) [58] where x_{12n} will be close to 1/2, while z_{6i} and z_{12n} will be close to 0 [55–57]. In this paper only five (3f, 4h, 12o, 12n and 6m) interstitial positions will be considered, unless otherwise stated.

In this section the relative stability of different structures, corresponding to the H atom occupation of different interstitial positions, will be explored in the case of YNi₅H and YNi₅H_{0.5} compositions.

From Figs. 4 and 5 it can be seen that the most stable position for the accommodation of hydrogen atoms is the 12n position, and that the 3f position is the second most stable. The 12n position was also found to be the most stable in the US-PP-GGA study on LaNi₅H_x [54], the FP linearized augmented plane wave (LAPW)-GGA study on LaNi₅H_x [59], the US-PP-GGA study on SmNi_{5-x}Ga_xH_y (on the SmNi₅H_x composition) [60] and the US-PP-GGA study on CaNi₅H_x [61] compounds.

We also note that the sequence of stability of different interstitial sites is the same for YNi₅H and YNi₅H_{0.5} compositions, and that it is identical to the sequences of stability previously found for CaNi₅H_x [61] and SmNi₅H_x [60] compounds.

In Fig. 4 the local coordination of interstitial sites is also indicated [16,52–54]. Although the 12n site is given in both tetrahedral (T) and octahedral (O) coordinations [16,52–54] in Fig. 4, it was found in previous studies [16,52–57,59,61] and in the present work (Tables 3, and S4 and S5 in Supplementary data) that the 12n site is very close to the 3f site. Therefore, it may be

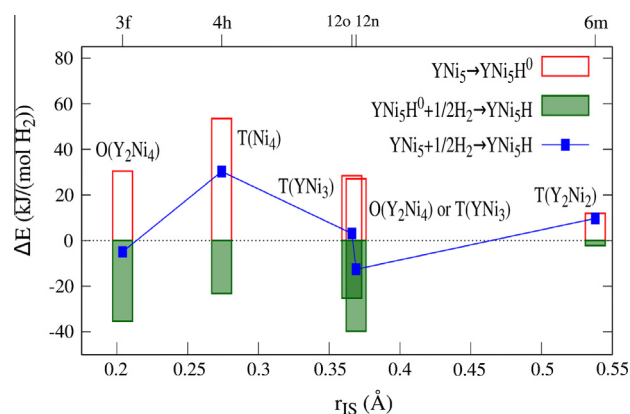


Fig. 4. Total energy changes for steps (1) $\text{YNi}_5 \rightarrow \text{YNi}_5\text{H}^0$ and (2) $\text{YNi}_5\text{H}^0 + 1/2\text{H}_2 \rightarrow \text{YNi}_5\text{H}$ as well as the full reaction $\text{YNi}_5 + 1/2\text{H}_2 \rightarrow \text{YNi}_5\text{H}$ vs. calculated radii (r_{IS}) of interstitial spheres for 3f, 4h, 12o, 12n and 6m sites in YNi₅. The local coordination of the interstitial sites is also provided [16,52–54]. Abbreviations: T-tetrahedral, O-octahedral.

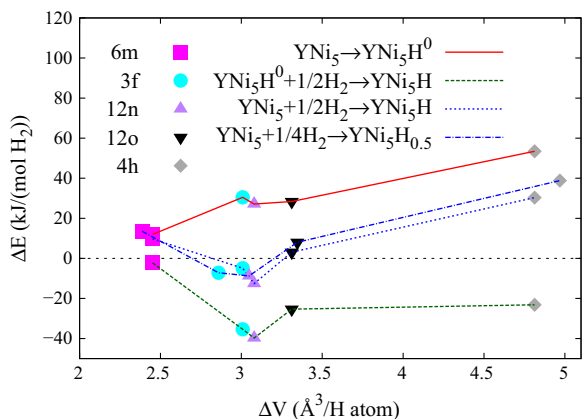


Fig. 5. Total energy changes for reactions $\text{YNi}_5 + 1/4\text{H}_2 \rightarrow \text{YNi}_5\text{H}_{0.5}$ and $\text{YNi}_5 + 1/2\text{H}_2 \rightarrow \text{YNi}_5\text{H}$, as well as the steps (1) $\text{YNi}_5 \rightarrow \text{YNi}_5\text{H}^0$ and (2) $\text{YNi}_5\text{H}^0 + 1/2\text{H}_2 \rightarrow \text{YNi}_5\text{H}$ vs. volume change $\Delta V = (V(\text{YNi}_5\text{H}_x) - V(\text{YNi}_5))/x$ for the 3f, 4h, 12o, 12n and 6m interstitial sites.

regarded as an octahedral site [54,61]. The coordinates of the five interstitial sites, as obtained for LaNi_5D_x compounds from neutron diffraction [16] (see, also, Table S1), also indicate that the 12n and 3f sites are close.

Although we are not aware of any neutron diffraction studies that were performed to determine the positions of H (D) atoms in YNi_5H_x compounds, it seems reasonable to compare the present results with neutron diffraction results obtained on the LaNi_5D_x [62–64,55,56] and CaNi_5D_x [65,66] compounds with low hydrogen (deuterium) content ($x < 1.0$). Results obtained in the present work, which show that H atoms prefer 12n and 3f sites that can be both regarded as octahedral sites [54], seem to be in accordance with these neutron diffraction studies, which also indicated a noticeable tendency of D atoms to occupy octahedral-like sites.

In the past the so-called Westlake geometrical approach [52,67] was used to explain the occupation of particular interstitial sites, the arrangement of H atoms and the maximum hydrogen content in metal hydrides. The model is based on the two criteria that should be met by stable hydrides [52,67]: a minimum radius of the interstitial hole of 0.4 Å and a minimum distance between H atoms of 2.1 Å.

Accordingly, whether there is a correlation between the energetics of formation of YNi_5H hydride and the size of the corresponding interstitial site will be investigated.

Following [68,69], the reaction $\text{YNi}_5 + 1/2\text{H}_2 \rightarrow \text{YNi}_5\text{H}$ will be resolved into two steps: (1) $\text{YNi}_5 \rightarrow \text{YNi}_5\text{H}^0$ and (2) $\text{YNi}_5\text{H}^0 + 1/2\text{H}_2 \rightarrow \text{YNi}_5\text{H}$. Step 1 is distortion and expansion of the YNi_5 structure to the arrangement of metal atoms in YNi_5H and step 2 is the insertion of the H atom into the expanded and distorted structure YNi_5H^0 . In Fig. 4 the total energy changes for the two steps are shown, together with total energy change for the full reaction vs. radii of interstitial spheres for the interstitial sites 3f, 4h, 12o, 12n and 6m.

Interstitial radii were calculated according to the procedure given in [53]. Additional comments about the calculation of interstitial sphere radii are given in the footnote.² The interstitial radii and atomic positions calculated from geometric conditions [53]

² The radii of interstitial spheres in YNi_5 are calculated according to [53] and the presently calculated lattice parameters $a = 4.889$ Å and $c = 3.956$ Å were used for their calculation. The 3f site is regarded as an octahedral site and its radius (i.e. the radius of the inscribed sphere) is calculated from the distance between the interstitial atom and the nearest metal atom [53]. Other interstitial sites are regarded as tetrahedral sites and the radius of the corresponding interstitial sphere is calculated from the requirement of the contact between this sphere and all metal atoms (i.e. corresponding spheres) at the vertices of the tetrahedron [53].

Table 2

Interstitial positions and radii calculated for YNi_5 according to the geometrical approach described in [53]. Lattice parameters used for the calculation of atomic positions and interstitial radii are those obtained from present DFT calculations: $a = 4.889$ Å and $c = 3.956$ Å.

Interstitial positions and radii in YNi_5				
Position	x	y	z	r_{IS} (Å)
3f	1/2	0	0	0.204
4h	1/3	2/3	0.374	0.274
12o	0.197	0.394	0.270	0.366
12n	0.394	0	0.120	0.369
6m	0.100	0.200	1/2	0.538

can be found in Table 2. It may be also noted from Table 2 that the 12n and 3f positions obtained from the geometrical approach seem to be more distant relative to the positions obtained from the present DFT calculations (Tables 3, S4 and S5).

The purpose of splitting the reaction $\text{YNi}_5 + 1/2\text{H}_2 \rightarrow \text{YNi}_5\text{H}$ into two steps is to analyse the two contributions and their relation to r_{IS} separately.

From the geometrical model [52,67] one would expect that interstitial sites with larger interstitial sphere radii will be more suitable for the accommodation of H atoms (i.e. the corresponding hydrides will be more stable) than those with smaller interstitial spheres.

Since the radius of the sphere inscribed in the octahedral 3f site is calculated differently from the radii of the spheres inscribed in other sites that are assumed to be tetrahedral ([53] and footnote²), tetrahedral sites will be discussed at first and the 3f site will be included in the discussion afterward.

From Fig. 4 it follows that the expected relation between ΔH and r_{IS} for tetrahedral sites is not fully obeyed. The 4h, 12o and 12n sites exhibit a trend that is in agreement with the geometrical model [52,67], while the 6m site deviates from this expected trend [52,67].

If, on the other hand, the contribution from the partial step $\text{YNi}_5 \rightarrow \text{YNi}_5\text{H}^0$ is examined with respect to the geometrical model [52,67], it can be observed that for the first step all tetrahedral sites (4h, 12o, 12n and 6m) follow the expected trend [52,67] (i.e. larger r_{IS} corresponds to the lower ΔE).

The octahedral 3f site deviates significantly from the trend followed by the other sites for both the full reaction $\text{YNi}_5 + 1/2\text{H}_2 \rightarrow \text{YNi}_5\text{H}$ and first step $\text{YNi}_5 \rightarrow \text{YNi}_5\text{H}^0$. As given in [53] and footnote², r_{IS} for the octahedral 3f site is calculated using different interatomic connections than for the tetrahedral sites, and this may be the reason for its deviating behaviour. It could be concluded that the effective volume of the 3f site is larger and that its ability to accommodate H atoms is higher than may be concluded from its r_{IS} .

The correlation between r_{IS} and total energy changes for step 2) $\text{YNi}_5\text{H}^0 + 1/2\text{H}_2 \rightarrow \text{YNi}_5\text{H}$ appear to be less obvious than the analogous correlation found for step 1.

In Fig. 5 total energy changes for reactions $\text{YNi}_5 + 1/4\text{H}_2 \rightarrow \text{YNi}_5\text{H}_{0.5}$, $\text{YNi}_5 + 1/2\text{H}_2 \rightarrow \text{YNi}_5\text{H}$ and steps (1) $\text{YNi}_5 \rightarrow \text{YNi}_5\text{H}^0$ and (2) $\text{YNi}_5\text{H}^0 + 1/2\text{H}_2 \rightarrow \text{YNi}_5\text{H}$ are given vs. $\Delta V = (V(\text{YNi}_5\text{H}_x) - V(\text{YNi}_5))/x$ for the five interstitial sites.

With the expected exception of the 3f site, ΔV values of particular interstitial sites follow the trend expected from the geometrical model [52,67], with a larger ΔV corresponding to a smaller r_{IS} (Table 2).

An interesting feature is shown in ΔE vs. ΔV for step 2. It consists of the dip in the total energy change vs. ΔV , which is located at the 12n (and close to the 3f) interstitial site. The same feature is also found in the overall energy change, ΔH vs. ΔV , for both reactions $\text{YNi}_5 + x/2\text{H}_2 \rightarrow \text{YNi}_5\text{H}_x$ ($x = 0.5, 1.0$). We also note that the same dip for the insertion of the H atom (step 2) and the overall

Table 3Optimized crystal structure parameters of YNi₅H hydrides with H atoms occupying interstitial 3f, 4h, 12o, 12n and 6m sites.

		<i>a</i> (Å)	<i>b</i> (Å)	<i>c</i> (Å)	α (°)	β (°)	γ (°)
YNi ₅ H ^{2f}		4.840	5.045	3.963	90.00	90.00	118.66
YNi ₅ H ^{4h}		4.982	4.982	4.034	90.00	90.00	120.00
YNi ₅ H ^{12o}		5.021	4.925	4.006	88.90	90.00	120.65
YNi ₅ H ¹²ⁿ		4.828	5.015	4.004	90.00	90.00	118.78
YNi ₅ H ^{6m}		5.000	4.921	3.980	90.00	90.00	120.54
	Y		Ni	Ni	Ni	Ni	H
YNi ₅ H ^{2f}	<i>x</i>	0.0000	0.3173	0.6827	0.5000	0.0000	0.5000
	<i>y</i>	0.0000	0.6347	0.3653	0.0000	0.5000	0.5000
	<i>z</i>	0.0000	0.0000	0.0000	0.5000	0.5000	0.5000
YNi ₅ H ^{4h}	<i>x</i>	0.0000	0.3333	0.6667	0.5076	−0.0151	0.5076
	<i>y</i>	0.0000	0.6667	0.3333	0.0151	0.4924	0.4924
	<i>z</i>	0.0016	−0.0217	0.0014	0.5058	0.5058	0.5058
YNi ₅ H ^{12o}	<i>x</i>	−0.0051	0.3393	0.6605	0.5012	−0.0070	0.5131
	<i>y</i>	−0.0101	0.6785	0.3210	0.0023	0.5061	0.5061
	<i>z</i>	−0.0220	0.0098	0.0109	0.5130	0.5164	0.5164
YNi ₅ H ¹²ⁿ	<i>x</i>	−0.0064	0.3122	0.6750	0.4936	−0.0064	0.4936
	<i>y</i>	0.0000	0.6372	0.3628	0.0000	0.5000	0.5000
	<i>z</i>	0.0055	0.0000	0.0000	0.5095	0.5032	0.5032
YNi ₅ H ^{6m}	<i>x</i>	−0.0023	0.3394	0.6621	0.4987	−0.0058	0.5062
	<i>y</i>	−0.0045	0.6787	0.3243	−0.0025	0.5004	0.5004
	<i>z</i>	0.0000	0.0000	0.0000	0.5000	0.5000	0.5000

reaction was also found in previous work on CaNi₅H_{*x*} hydrides [61]. This dip is probably a consequence of the well known fact that at some optimum interatomic distance the total energy will exhibit a minimum (i.e. that cohesion will be at its maximum) [70]. Finally, we note that the ΔV value that corresponds to the dip is about 3.0 Å³/(H atom) for $x = 0.5$ and 3.1 Å³/(H atom) for $x = 1.0$ and that this value is in a good agreement with the value of 2.9 Å³/(H atom) given by the rule extracted from experimental observations [71].

After the site preference of H atoms in the YNi₅ metal matrix has been determined, the stability of the α solid solution can be discussed. It should be noted that the pressure–composition isotherms given in [7,9,10] have certain discrepancies in their results. According to [7], in the approximate interval of $0 < x < 2.5$ ($x = n(\text{H})/n(\text{YNi}_5)$) there are three different hydride phases and two two-phase coexistence regions at 294 K. According to the absorption isotherms measured in [9,10] that were measured at 248 K and 296 K, respectively, there are only two hydride phases and one two-phase coexistence region in the approximate intervals of $0 < x < 3.0$ (at 248 K) and $0 < x < 4.5$ (at 296 K). The boundary of the region of the α solid solution would be roughly at about $x = 0.5$ at 296 K [10] (or lower at 248 K [9]). It should be noted that there is a significant difference between the absorption and desorption isotherms measured at the same temperatures in [9,10], and that two-phase coexistence region (indicated by pressure plateaux) found in one isotherm could be absent in the other. Isotherm given in [7] indicates that the border of the region of the α solid solution would be lower than $x = 0.5$ at 294 K.

If not stated otherwise, in this work we assume that, in accordance with [9,10], only two phases and one two-phase coexistence region exist in the approximate interval of $0 < x < 4.5$ at low temperatures.

To investigate how the enthalpy of formation of the α solid solution depends on the composition, a composition with $x = 0.25$ was modelled. The H atom was placed, according to the above results, at the 12n site (YNi₅H_{0.25}¹²ⁿ or Y₄Ni₂₀H¹²ⁿ). The enthalpies of formation of YNi₅H_{*x*}¹²ⁿ hydrides, $\Delta H_{0,0 \rightarrow x}$, calculated in the present work are −4.4 kJ/(mol H₂), −8.8 kJ/(mol H₂) and −12.6 kJ/(mol H₂) for $x = 0.25, 0.5$ and 1.0, respectively. To the best of our knowledge, a corresponding value that could be obtained either from experiment or from some other theoretical study is not available at present.

3.3. YNi₅H_{*x*} ($x = 3.0, 3.5, 4.0$) compounds and the $\alpha \rightarrow \beta$ reaction

The pressure–composition isotherms given in [10] indicate that a single phase region of the β -phase extends approximately in the region of about $x \geq 4.5$, while the two phase α – β region is found approximately between $0.5 \leq x \leq 4.5$, at 296 K.

Since the crystal structure of the YNi₅H_{*x*} hydrides is, to the best of our knowledge, not known at present, in order to model the crystal structure of YNi₅H_{*x*} compounds with $x \geq 3.0$, the crystal structures of the β^I -LaCo₅D_{3.35} and β^{III} -CeCo₅D_{2.55} phases [17] were used in the present work.

In Table S2 the crystal structure parameters, as determined from a neutron diffraction experiment on a β^I -LaCo₅D_{3.35} compound [17], are provided. Three different compositions were modelled, namely YNi₅H_{3.0}, YNi₅H_{3.5} and YNi₅H_{4.0}. According to [17] (see, also, Table S2) a full occupancy of D positions in β^I phase deuteride LaCo₅D_{*x*} would result in the composition LaCo₅D₄ or, analogously, in the YNi₅H₄ composition in the case of YNi₅H_{*x*} compounds. Therefore, these data were used to model the YNi₅H₄ composition in the present study, and the corresponding crystal structure parameters obtained in the present calculations are given in Table 4. The conventional unit cell of the β^I phase LaCo₅D_{3.35} is base centred orthorhombic, containing two f.u., and the primitive unit cell contains one f.u. Therefore, hydrides with lower hydrogen contents can be realised either by removing one H atom from one of the two crystallographic H positions in the conventional unit cell (Y₂Ni₁₀H₇ or YNi₅H_{3.5} composition), or by removing one H atom

Table 4Optimized crystal structure parameters of the YNi₅H₄ compound.

YNi ₅ H ₄ (space group Cmmm)				
<i>a</i> (Å)		<i>b</i> (Å)	<i>c</i> (Å)	
8.729		5.259	4.032	
Atom	Position	<i>x</i>	<i>y</i>	<i>z</i>
Y	2a	0.0000	0.0000	0.0000
Ni1	4g	0.3592	0.0000	0.0000
Ni2	2c	0.5000	0.0000	0.5000
Ni3	4f	0.2500	0.2500	0.5000
H1	4e	0.2500	0.2500	0.0000
H2	4h	0.1380	0.0000	0.5000

from one of the two crystallographic H positions in the primitive unit cell (YNi₅H_{3.0} composition). It should be determined whether the removal of the H atom from the 4e or from the 4h position will result in a more stable structure. For both YNi₅H_{3.5} and YNi₅H_{3.0} compositions it was found that removal from the 4e position results in a more stable structure, with energy differences of 6.3 kJ/(mol H₂) and 14.5 kJ/(mol H₂), respectively. Therefore, for both YNi₅H_{3.5} and YNi₅H_{3.0} compositions with crystal structures modelled on the basis of the β^l phase LaCo₅D_{3.35}, structures with one atom removed from the 4e position in the conventional and primitive unit cell, respectively, will be used for the calculation of the enthalpies of formation.

As an additional model for the YNi₅H_{3.0} composition, crystal structure data of the β^{III}-CeCo₅D_{2.55} phase [17] (see Table S3) with H occupancies set to 1.0 were used in the present work, and the corresponding crystal structure parameters obtained are given in Table 5.

Since there are two crystal structure models that represent the YNi₅H_{3.0} composition, it is necessary to compare their relative stability. The structure modelled on the basis of the β^{III}-CeCo₅D_{2.55} phase is more stable by 1.5 kJ/(mol H₂) than the structure modelled on the basis of the β^l-LaCo₅D_{3.35} phase.

In Table 6 the enthalpies of formation corresponding to the reaction (1) obtained from non-spin-polarized calculations are given. The previous experimental result [10], which provides the enthalpy of formation of the β phase from the α phase and molecular hydrogen according to the reaction (1), is also given in Table 6.

Different starting and ending compositions and the corresponding structural models are used for the calculation of the

corresponding enthalpies for two reasons, these being to model each phase with more than one model to hopefully employ an approximately appropriate model and to examine the sensitivity of results on the different structural models used for the calculations.

From the examination of the enthalpies calculated in the present work, and given in Table 6, it can be seen that their values lie in a relatively narrow range of −16.9 to −21.6 kJ/(mol H₂), demonstrating that the enthalpy is not too sensitive to the details of the model used for its calculation. Moreover, the borders of this interval of calculated values correspond to 77% and 99% of the experimentally determined value of −21.9 ± 1.7 kJ/(mol H₂), respectively [10].

If one reduces the considered phases to those that contain hydrogen (i.e. if one removes x₁ = 0.0 for the α phase) in Table 6, the set of values given in Table 6 is then reduced to the interval −17.7 to −21.6 kJ/(mol H₂), and these borders correspond to 81% and 99% of the experimental value, respectively [10].

3.4. Inclusion of zero-point energy corrections

The theoretical results obtained in the present work and discussed above do not include zero-point energy (ZPE) corrections. According to the calculations of the ZPE in LaNi₅H compounds with H atoms in the 12n, 6m, 12o and 4h positions, the ZPE of LaNi₅H¹²ⁿ was found to be the lowest among considered interstitial positions [73]. Therefore, we believe that our conclusion that H atom will occupy the 12n position in the case of YNi₅H_x (x = 0.25, 0.5, 1.0) compounds will not change after inclusion of ZPE corrections.

To check the possible influence of ZPE corrections on the energetics of the α → β reaction, phonon spectra were calculated for YNi₅, H₂ and YNi₅H₄ in the β^l-LaCo₅D_{3.35} (i.e. β^l-LaCo₅D_{4.0}) phase structure [17] using density functional perturbation theory (DFPT) [74–76]. In the case of YNi₅, the calculated ZPE was 19.1 kJ/(mol YNi₅). The calculated vibrational frequency of the H₂ molecule was found to be ω = 4337 cm^{−1} (corresponding to a ZPE of 25.9 kJ/(mol H₂)), compared to a previously calculated DFT value of 4399 cm^{−1} [77] and experimental value of 4405 cm^{−1} [77]. However, in the case of YNi₅H₄ imaginary frequencies were found, indicating a structural instability in this compound. It seems that this finding is in agreement with previous DFT calculations on isostructural compound LaCo₅H₄, where structural instabilities were also detected [77]. The two imaginary frequencies correspond almost entirely to the vibrations of the two H atoms on the 4e positions (space group Cmmm), that are located at the centres of

Table 5
Optimized crystal structure parameters of the YNi₅H₃ compound.

YNi ₅ H ₃ (space group Cccm)				
a (Å)	b (Å)	c (Å)		
8.615	5.125	8.048		
Atom	Position	x	y	z
Y	4c	0.0000	0.0000	0.0000
Ni1	8l	0.3477	0.9694	0.0000
Ni2	4b	0.5000	0.0000	0.2500
Ni3	8k	0.2500	0.2500	0.2394
H1	4e	0.2500	0.2500	0.0000
H2	8g	0.1354	0.0000	0.2500

Table 6
Results of non-spin-polarized calculations for the enthalpies of formation for the reaction (1). The previous experimental result [10] is also provided for comparison.

ΔH (kJ/(mol H ₂))	
<i>Present results</i>	
ΔH _{0.0–3.0} ^a	−17.9 ^a
ΔH _{0.0–3.0} ^b	−19.5 ^b
ΔH _{0.0–3.5} ^a	−17.0 ^a
ΔH _{0.0–4.0} ^a	−16.9 ^a
ΔH _{0.25–3.0} ^a	−19.1 ^a
ΔH _{0.25–3.0} ^b	−20.8 ^b
ΔH _{0.25–3.5} ^a	−18.0 ^a
ΔH _{0.25–4.0} ^a	−17.7 ^a
ΔH _{0.5–3.0} ^a	−19.7 ^a
ΔH _{0.5–3.0} ^b	−21.6 ^b
ΔH _{0.5–3.5} ^a	−18.4 ^a
ΔH _{0.5–4.0} ^a	−18.0 ^a
<i>Previous experimental result</i>	
ΔH _{α→β}	−21.9 ± 1.7 [10]

^a This value was obtained using β^l-LaCo₅D_{3.35} phase [17] as a model for the corresponding YNi₅H_x composition.

^b This value was obtained using β^{III}-CeCo₅D_{2.55} phase [17] as a model for the YNi₅H_{3.0} composition.

Table 7
Optimized crystal structure parameters of the YNi₅H₄ compound (β^l-LaCo₅D_{4.0}-like structure) with the initial positions of the H atoms shifted to avoid imaginary modes.

YNi ₅ H ₄			
a (Å)	b (Å)	c (Å)	
4.129	5.041	5.041	
α (°)		β (°)	
61.79		90.00	
Atom	x	y	z
Y	0.0430	0.0400	0.0400
Ni	0.0013	0.3958	0.3958
Ni	0.0013	0.6842	0.6842
Ni	0.5076	0.5400	0.5400
Ni	0.5177	0.5400	0.0400
Ni	0.5177	0.0400	0.5400
H	0.1105	0.5402	0.0400
H	0.1105	0.0400	0.5402
H	0.5451	0.1749	0.1749
H	0.5453	0.9050	0.9050

the Y_2Ni_4 octahedra. In the case of the $P6/mmm$ space group these correspond to the 3f positions and this result is also in agreement with previous DFT analysis of the vibrational properties of H atoms in $LaNi_5H_x$ compounds, where it was found that the interstitial 3f position does not correspond to the local minimum of total energy [57].

We have performed additional geometry optimization of the YNi_5H_4 composition with H atoms shifted from their positions. This resulted in a structure (Table 7) without imaginary frequencies, that was more stable by 4.2 kJ/(mol H_2) than the structure that used the initial crystal structure parameters obtained in [17]. If this structure is used as a model of the β phase, theory is brought in even closer agreement with experiment, with $\Delta H_{0.25-4.0'} = -22.2$ kJ/(mol H_2) and $\Delta H_{0.5-4.0'} = -22.8$ kJ/(mol H_2), compared to the experimental value of -21.9 ± 1.7 [10].

The calculated ZPE for this additionally relaxed YNi_5H_4 compound was 89.8 kJ/(mol YNi_5H_4), and the ZPE change for the reaction $YNi_5 + 2H_2 \rightarrow YNi_5H_4$ is then $\Delta E_{ZPE} = 9.4$ kJ/(mol H_2). This value can be used to approximately correct the above values for the enthalpies of formation, giving approximate ZPE corrected (AZPEC) values of $\Delta H_{0.25-4.0'}^{AZPEC} = -12.8$ kJ/(mol H_2) and $\Delta H_{0.5-4.0'}^{AZPEC} = -13.4$ kJ/(mol H_2). The inclusion of the ZPE correction, therefore, degrades the agreement between the present theoretical results and experiment, resulting in theoretical values of about 58% and 67% of the experimental value [10].

4. Conclusion

DFT calculations were performed for YNi_5H_x compounds with $x = 0.0, 0.25, 0.5, 1.0, 3.0, 3.5, 4.0$. The calculations employed ultra-soft pseudopotentials and a plane wave basis set. The formation energetics and the preference of H atoms for particular interstitial sites was explored for the YNi_5H_x compounds.

It was found that H atoms prefer the 12n (and 3f) interstitial sites, in accordance with previous experimental and theoretical studies on the hydrides (deuterides) of isostructural ANi_5 compounds in which H (D) atoms were found to preferentially occupy octahedral-like sites.

The obtained results are analysed with respect to a geometrical model [52,67], and certain correlations were found between the radii of interstitial spheres and the total energy changes that occur in the specific abstract steps of the formation of the hydrides, as well as the corresponding enthalpies of formation.

The crystal structures of the α and β phases were modelled and the enthalpy of formation for the $\alpha \rightarrow \beta$ reaction was calculated. Calculated values for the enthalpy of formation for the $\alpha \rightarrow \beta$ reaction were found to be in reasonable agreement with a value previously obtained from experiment.

Acknowledgments

Calculations in this work have been done using the QUANTUM ESPRESSO package [13]. For the visualization of crystal structures the VESTA program [72] was employed.

Computational resources were provided by the Isabella cluster (isabella.srce.hr) at the Zagreb University Computing Centre (Srce).

The support for this research from the Ministry of Science, Education and Sport of the Republic of Croatia under Project No. 098-0982904-2941 is highly appreciated.

Appendix A. Supplementary material

Supplementary data associated with this article can be found, in the online version, at <http://dx.doi.org/10.1016/j.jallcom.2014.10.106>.

References

- [1] K.H.J. Buschow, Rep. Prog. Phys. 40 (1977) 1179–1256.
- [2] H.H. Van Mal, Philips Res. Rep. Suppl. (1976) 1–88.
- [3] M.H. Mendelssohn, D.M. Gruen, A.E. Dwight, Nature 269 (1977) 45–47.
- [4] J.L. Anderson, T.C. Wallace, A.L. Bowman, C.L. Radosevich, M.L. Courtney, LA-5320-MS Informal Report, Los Alamos Scientific Laboratory, 1973.
- [5] T. Takeshita, W.E. Wallace, R.S. Craig, Inorg. Chem. 13 (1974) 2282–2283.
- [6] V.K. Sarynin, V.V. Burnasheva, K.N. Semenenko, Izv. Akad. Nauk SSSR, Met. 4 (1977) 69–70.
- [7] T. Takeshita, K.A. Gschneidner Jr., J.F. Lakner, J. Less-Common Met. 78 (1981) 43–47.
- [8] B. Šorgić, Ž. Blažina, A. Drašner, J. Alloy. Compd. 265 (1998) 185–189.
- [9] H. Senoh, T. Yonei, H.T. Takeshita, N. Takeichi, H. Tanaka, N. Kuriyama, Mater. Trans. 46 (2005) 152–154.
- [10] S. Mitrokhin, T. Zotov, E. Movlaev, V. Verbetsky, J. Alloy. Compd. 446–447 (2007) 603–605.
- [11] D. Vanderbilt, Phys. Rev. B 41 (1990) 7892–7895.
- [12] We used the pseudopotentials Y.pbe-nsp-van.UPF, Ni.pbe-nd-rrkjus.UPF and H.pbe-rrkjus.UPF from <http://www.quantum-espresso.org>.
- [13] P. Giannozzi, S. Baroni, N. Bonini, M. Calandra, R. Car, C. Cavazzoni, D. Ceresoli, G.L. Chiarotti, M. Cococcioni, I. Dabo, A. Dal Corso, S. De Gironcoli, S. Fabris, G. Fratesi, R. Gebauer, U. Gerstmann, C. Gougoussis, A. Kokalj, M. Lazzeri, L. Martin-Samos, N. Marzari, F. Mauri, R. Mazzarello, S. Paolini, A. Pasquarello, L. Paulatto, C. Sbraccia, S. Scandolo, G. Sclauzero, A.P. Seitsonen, A. Smogunov, P. Umari, R.M. Wentzcovitch, J. Phys. Condens. Matter 21 (2009) 395502.
- [14] J.P. Perdew, K. Burke, M. Ernzerhof, Phys. Rev. Lett. 77 (1996) 3865–3868.
- [15] J.P. Perdew, K. Burke, M. Ernzerhof, Phys. Rev. Lett. 78 (1997) 1396–1396.
- [16] A. Percheron-Guegan, C. Lartigue, J.C. Achard, P. Germin, F. Tasset, J. Less-Common Met. 74 (1980) 1–12.
- [17] F.A. Kuijpers, B.O. Loopstra, J. Phys. Chem. Solids 35 (1974) 301–306.
- [18] H.J. Monkhorst, J.D. Pack, Phys. Rev. B 13 (1976) 5188–5192.
- [19] N. Marzari, D. Vanderbilt, A. De Vita, M.C. Payne, Phys. Rev. Lett. 82 (1999) 3296–3299.
- [20] J.J. Murray, M.L. Post, J.B. Taylor, J. Less-Common Met. 90 (1983) 65–73.
- [21] C. Ortiz, O. Eriksson, M. Klintonberg, Comput. Mater. Sci. 44 (2009) 1042–1049.
- [22] <http://gurka.fysik.uu.se/ESP> (accessed 5.12.2013).
- [23] G.E. Grechnev, A.V. Logosha, A.S. Panfilov, A.G. Kuchin, A.N. Vasijev, Low Temp. Phys. 37 (2011) 138–143.
- [24] Y.V. Knyazev, A.V. Lukoyanov, Y.I. Kuz'min, A.G. Kuchin, Opt. Spectrosc. 111 (2011) 808–813.
- [25] T. Suenobu, I. Tanaka, H. Adachi, G.-y. Adachi, J. Alloy. Compd. 221 (1995) 200–206.
- [26] H. Yukawa, Y. Takahashi, M. Morinaga, Intermetallics 4 (1996) S215–S224.
- [27] H. Yukawa, M. Morinaga, Adv. Quant. Chem. 29 (1998) 83–108.
- [28] J.C. Crivello, M. Gupta, J. Alloy. Compd. 404–406 (2005) 565–569.
- [29] M. Morinaga, H. Yukawa, Mater. Sci. Eng. A 329–331 (2002) 268–275.
- [30] K. Nakatsuka, M. Yoshino, H. Yukawa, M. Morinaga, J. Alloy. Compd. 293 (1999) 222–226.
- [31] A. Jain, G. Hautier, C.J. Moore, S. Ping Ong, C.C. Fischer, T. Mueller, K.A. Persson, G. Ceder, Comput. Mater. Sci. 50 (2011) 2295–2310.
- [32] A. Jain, G. Hautier, S.P. Ong, C.J. Moore, C.C. Fischer, K.A. Persson, G. Ceder, Phys. Rev. B 84 (2011).
- [33] A. Jain, S.P. Ong, G. Hautier, W. Chen, W.D. Richards, S. Dacek, S. Cholia, D. Gunter, D. Skinner, G. Ceder, K. Persson, APJ Mater. 1 (2013) 011002.
- [34] <The Materials Project, <http://materialsproject.org/>> (accessed 5.12.2013).
- [35] W. Setyawan, S. Curtarolo, Comput. Mater. Sci. 49 (2010) 299–312.
- [36] S. Curtarolo, W. Setyawan, S. Wang, J. Xue, K. Yang, R.H. Taylor, L.J. Nelson, G.L.W. Hart, S. Sanvito, M. Buongiorno-Nardelli, N. Mingo, O. Levy, Comput. Mater. Sci. 58 (2012) 227–235.
- [37] <http://afloplib.org> (accessed 5.12.2013).
- [38] <http://alloy.phys.cmu.edu> (accessed 5.12.2013).
- [39] D. Gignoux, D. Givord, A. Del Moral, Solid State Commun. 19 (1976) 891–894.
- [40] M. Coldea, D. Andreica, M. Bitu, V. Crisan, J. Magn. Magn. Mater. 157–158 (1996) 627–628.
- [41] E. Burzo, V. Pop, I. Costina, J. Magn. Magn. Mater. 157–158 (1996) 615–616.
- [42] I. Kitagawa, K. Terao, M. Aoki, H. Yamada, J. Phys. Condens. Matter 9 (1997) 231–239.
- [43] G.I. Miletić, Ž. Blažina, J. Alloy. Compd. 335 (2002) 81–90.
- [44] A. Kuchin, A. Ermolenko, V. Khrabrov, G. Makarova, E. Belozherov, J. Magn. Magn. Mater. 159 (1996) L309–L312.
- [45] G.E. Grechnev, A.V. Logosha, I.V. Svechikarev, A.G. Kuchin, Y.A. Kulikov, P.A. Korzhavyi, O. Eriksson, Low Temp. Phys. 32 (2006) 1140–1146.
- [46] A. Bajorek, D. Stysiak, G. Chełkowska, J. Deniszczczyk, W. Borgiel, M. Neumann, Mater. Sci.-Pol. 24 (2006) 867–874.
- [47] A. Pasturel, C. Colinet, C. Allibert, P. Hicter, A. Percheron-Guegan, J.C. Achard, Phys. Status Solidi B 125 (1984) 101–106.
- [48] P.R. Subramanian, J.F. Smith, Metall. Trans. B 16 (1985) 577–584.
- [49] A.K. Niessen, A.R. Miedema, F.R. de Boer, R. Boom, Phys. B 152 (1988) 303–346.
- [50] A.R. Miedema, R. Boom, F.R. de Boer, J. Less-Common Met. 41 (1975) 283–298.
- [51] A.R. Miedema, P.F. de Châtel, F.R. de Boer, Phys. B+C 100 (1980) 1–28.
- [52] D.G. Westlake, J. Less-Common Met. 91 (1983) 275–292.
- [53] K.J. Gross, A. Züttel, L. Schlapbach, J. Alloy. Compd. 274 (1998) 239–247.

- [54] K. Tatsumi, I. Tanaka, H. Inui, K. Tanaka, M. Yamaguchi, H. Adachi, *Phys. Rev. B* 64 (2001) 1841051–18410510.
- [55] H. Hayakawa, K. Nomura, Y. Ishido, E. Akiba, S. Shin, H. Asano, F. Izumi, N. Watanabe, *J. Less-Common Met.* 143 (1988) 315–324.
- [56] E.H. Kisi, E.MacA. Gray, S.J. Kennedy, *J. Alloy. Compd.* 216 (1994) 123–129.
- [57] A. Tezuka, H. Wang, H. Ogawa, T. Ikeshoji, *Phys. Rev. B* 81 (2010) 1343041–1343047.
- [58] T. Hahn, in: *Space-Group Symmetry, International Tables for Crystallography*, Wiley, 2005.
- [59] C. Zhang, T. Gao, X. Qi, Y. Zhang, L. Tang, J. Zhou, B. Chen, *Phys. B* 403 (2008) 2372–2382.
- [60] N. Biliškov, G.I. Miletić, A. Drašner, *Int. J. Hydrog. Energy* 38 (2013) 12213–12222.
- [61] G.I. Miletić, A. Drašner, *J. Alloy. Compd.* 582 (2014) 466–474.
- [62] P. Fischer, A. Furrer, G. Busch, L. Schlapbach, *Helv. Phys. Acta* 50 (1977) 421–430.
- [63] R. Hempelmann, D. Richter, G. Eckold, J.J. Rush, J.M. Rowe, M. Montoya, *J. Less-Common Met.* 104 (1984) 1–12.
- [64] J.L. Soubeyroux, A. Percheron-Guegan, J.C. Achard, *J. Less-Common Met.* 129 (1987) 181–186.
- [65] A. Yoshikawa, Y. Uyenishi, H. Iizumi, T. Matsumoto, N. Takano, F. Terasaki, *J. Alloy. Compd.* 280 (1998) 204–208.
- [66] L.D. Calvert, B.M. Powell, J.J. Murray, Y. Le Page, *J. Solid State Chem.* 60 (1985) 62–67.
- [67] D.G. Westlake, *J. Less-Common Met.* 90 (1983) 251–273.
- [68] K. Miwa, A. Fukumoto, *Phys. Rev. B* 65 (2002) 1551141–1551147.
- [69] H. Smithson, C.A. Marianetti, D. Morgan, A. Van der Ven, A. Predith, G. Ceder, *Phys. Rev. B* 66 (2002) 1441071–14410710.
- [70] W.A. Harrison, *Electronic Structure and the Properties of Solids: the Physics of the Chemical Bond*, Dover Books on Physics, Dover Publications, New York, 1989.
- [71] B. Baranowski, S. Majchrzak, T.B. Flanagan, *J. Phys. F: Met. Phys.* 1 (1971) 258–261.
- [72] K. Momma, F. Izumi, *J. Appl. Cryst.* 44 (2011) 1272–1276.
- [73] S. Saito, M. Katagiri, V. Tserolas, J. Nakamura, H. Onodera, H. Ogawa, in: *Mater. Res. Soc. Symp. Proc.*, vol. 1216, 2010, pp. 1216-W03-01.
- [74] S. Baroni, P. Giannozzi, A. Testa, *Phys. Rev. Lett.* 58 (1987) 1861–1864.
- [75] S. Baroni, S. De Gironcoli, A. Dal Corso, P. Giannozzi, *Rev. Mod. Phys.* 73 (2001) 515–562.
- [76] X. Gonze, *Phys. Rev. A* 52 (1995) 1096–1114.
- [77] J.F. Herbst, L.G. Hector Jr., *J. Alloys Compd.* 446–447 (2007) 188–194.